



# Recent Advancement in Boron-Based Efficient and Pure Blue Thermally Activated Delayed Fluorescence Materials for Organic Light-Emitting Diodes

Hyuna Lee<sup>†</sup>, Durai Karthik<sup>†</sup>, Raju Lampande<sup>†</sup>, Jae Hong Ryu and Jang Hyuk Kwon\*

Organic Optoelectronic Device Laboratory, Information Display Department, Kyung Hee University, Seoul, South Korea

## OPEN ACCESS

### Edited by:

Chihaya Adachi,  
Kyushu University, Japan

### Reviewed by:

Takuji Hatakeyama,  
Kwansei Gakuin University, Japan  
Jian Fan,  
Soochow University, China

### \*Correspondence:

Jang Hyuk Kwon  
jhkwon@khu.ac.kr

<sup>†</sup>These authors have contributed  
equally to this work

### Specialty section:

This article was submitted to  
Organic Chemistry,  
a section of the journal  
Frontiers in Chemistry

Received: 14 February 2020

Accepted: 09 April 2020

Published: 19 May 2020

### Citation:

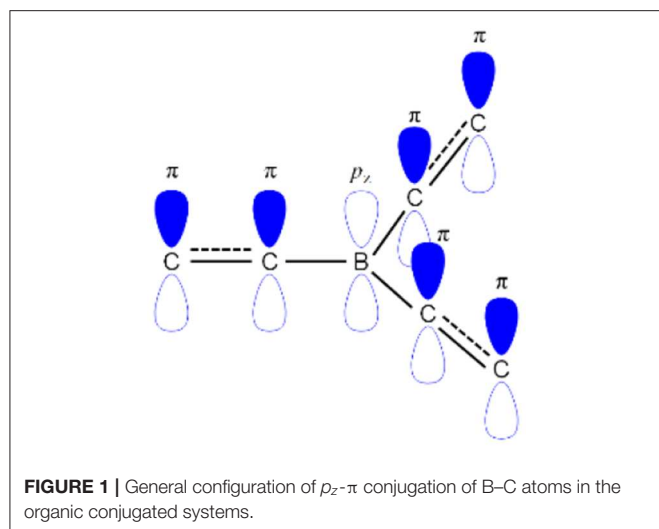
Lee H, Karthik D, Lampande R,  
Ryu JH and Kwon JH (2020) Recent  
Advancement in Boron-Based  
Efficient and Pure Blue Thermally  
Activated Delayed Fluorescence  
Materials for Organic Light-Emitting  
Diodes. *Front. Chem.* 8:373.  
doi: 10.3389/fchem.2020.00373

In the last few years, electron-deficient materials have been actively researched for application in organic light-emitting diode (OLED) as dopant and electron-transporting materials. The boron-containing materials are interesting as they give good emissive properties in solid state with an electron-accepting character. Recently, many boron-containing materials are used as emissive materials for thermally activated delayed fluorescence (TADF) OLED applications. In this review, boron acceptor-based push-pull small molecules used for application in blue TADF OLEDs are reviewed, covering their different types of acceptor, molecular design, structure-property relation, material properties, and device properties. Also, the importance of boron acceptors to address the key issue of blue TADF OLEDs is discussed.

**Keywords:** boron acceptor, thermally activated delayed fluorescence (TADF), multiple resonance, electroluminescence, blue organic light-emitting diode (OLED)

## INTRODUCTION

Organic light-emitting diodes (OLEDs) have been actively investigated in the last three decades since the first discovery by Tang and Vanslyke (1987) because of their incomparable advantages as they offer low power consumption, high brightness, color purity, light weight, large viewing angle, and flexible nature compared to other lighting sources. The first-generation fluorescent OLEDs exhibited lower efficiency due to usage of only 25% of singlet excitons formed during the exciton recombination process. Later, second-generation OLEDs were developed to utilize both singlet and triplet excitons to increase the internal quantum efficiency (IQE) up to 100% using heavy metal atoms, which are also called phosphorescent OLEDs (Baldo et al., 1998). Though the efficiency, color purity, and device lifetime of phosphorescent green and red OLEDs are satisfactory to commercialize, blue phosphorescent OLEDs suffer from low efficiency, poor color purity, and short device lifetime due to high triplet energy of blue emitters (Scholz et al., 2015; Im et al., 2017). Later, third-generation OLEDs were demonstrated with 100% IQE by using the concept of thermally activated delayed fluorescence (TADF) process in pure organic materials (Uoyama et al., 2012). These TADF materials are promising to achieve high efficiency and color purity in the blue OLEDs. Thus, recently, many reports were published on blue TADF emitters based on different types of donor and acceptor design concepts (Liang et al., 2019).



The boron-based materials have received tremendous interest in the last few years as they are widely used as potential candidates in the optoelectronic devices (Entwistle and Marder, 2004; Turkoglu et al., 2017; Mellerup and Wang, 2019). Boron atom has a vacant  $p$ -orbital which gives an electron-deficient nature or Lewis acidic nature (Brown and Dodson, 1957). This electron-deficient boron can make a  $\pi$ -conjugation with organic conjugated system through empty  $p_z$  orbital of boron and  $\pi$ -orbital of carbon as shown in **Figure 1**. Recently, boron-based materials have drawn immense attraction in designing as new TADF acceptor moieties because they offer excellent photophysical and electrochemical properties. Especially, boron materials show high photoluminescence quantum yield (PLQY) because of their  $sp^2$  hybridized trigonal planar geometry which gives rigid/planar molecular structure resulting in less non-radiative decay (Yamaguchi and Wakamiya, 2006; Elbing and Bazan, 2008; Von Grotthuss et al., 2018). Generally, boron-containing materials exhibit largely blue emission due to their weak acceptor nature, which yields a large band gap. Though the boron atom has a weak acceptor nature, boron acceptor materials have exhibited different color emissions varying from blue to red depending on the acceptor design strategy (D'aleo et al., 2017; Yang et al., 2018; Zhang et al., 2019). Not only the tri-coordinate boron shows excellent emission properties, but the tetra-coordinate boron also shows very good emissive properties as evident from BODIPY (boron-dipyrromethene) materials (Bonardi et al., 2008; Schellhammer et al., 2017; Stachelek et al., 2017; Zampetti et al., 2017). Unlike tri-coordinate boron, one important thing in tetra-coordinate boron is to keep the charge neutral of overall material by forming a covalent bond with mono-anionic chelate ligand to dissipate boron's negative charge. Therefore, the rigidity of the molecule is enhanced by virtue of chelation effect resulting in good emissive properties (Frath et al., 2014).

Recently, many TADF materials with boron acceptors have been reported with good performances. There are several boron TADF materials available in the literature for different color OLEDs. However, blue TADF OLEDs are interesting as they are promising alternatives to commercial fluorescent blue emitters.

As boron-based blue TADF materials are promising to realize high efficiency with a long lifetime, the detailed knowledge on the structure–property relation and design tactics of boron-based blue TADF emitters is highly desirable. Thus, in this review, we focus on the boron acceptor-based materials used for blue TADF OLEDs. Also, we discuss the requirements of blue emitters and different types of boron acceptors (tri- and tert-coordinate boron) used for blue TADF materials. In addition, we also discuss multiple resonance TADF materials and their underlying mechanism which is particularly for boron blue TADF OLEDs. Finally, the future outlook summarizes to achieve high efficiency and long lifetime for boron-based blue TADF OLEDs.

## BASIC REQUIREMENT OF BLUE MATERIALS

Over the last few years, huge progress has been made on the synthesis of new blue TADF emitters for OLED applications. To use blue TADF material for OLED applications that should be capable of making high external quantum efficiency (EQE), low-efficiency roll-off, good color purity of  $x < 0.15$ ,  $y < 0.10$ , and a long lifetime. To make OLED containing these properties, blue TADF material should have a high PLQY, wide energy gap ( $\Delta E_{ST}$ ) between highest occupied molecular orbital (HOMO) and lowest unoccupied molecular orbital (LUMO), small  $\Delta E_{ST}$  between the lowest singlet and triplet states, fast reverse intersystem crossing (RISC) from triplet to singlet, narrow full width at half maximum (FWHM), and high horizontal dipole orientation in the film.

Normally, small  $\Delta E_{ST}$  can be achieved by reducing an exchange integral between HOMO and LUMO and a large twist angle between the donor and the acceptor. The use of a rigid and symmetric structure supports to enhance PLQY and to achieve a narrow FWHM. The high bandgap ( $S_1$ ) energy can be reached by applying short  $\pi$ -conjugation length and the donor-acceptor interaction. The high horizontal orientation of the emitter molecule in the film is important to achieve high light out-coupling efficiency. Generally, blue TADF OLED shows the poor lifetime because of the long-delayed exciton lifetime of the emitter. Therefore, short-delayed exciton lifetime is highly required for achieving a long lifetime and high-efficiency OLEDs.

## SEVERAL BORON CHEMICAL STRUCTURES VS. THEIR PERFORMANCES

### Unbridged Boron-Type Acceptor for Blue Thermally Activated Delayed Fluorescence Emitters

Triarylboron compounds have been used as optoelectronic materials due to their electron-withdrawing abilities. In 2015, Suzuki et al. (2015) firstly reported a series of triarylboron-based TADF emitters, **2DAC-Mes<sub>3</sub>B** and **DAC-Mes<sub>3</sub>B**, by introducing amine-based electron donors. Methyl groups at the *ortho* position of C-B bonds protect the centered boron atom from hydrolysis by oxygen and water. They attached bis(diphenylamino)carbazole (2DAC) and diphenylaminocarbazole (DAC) moieties for electron-donating groups. The **2DAC-Mes<sub>3</sub>B** and **DAC-Mes<sub>3</sub>B**

showed sky-blue and blue emission peaks at 487 and 477 nm in 16 wt% doped (Bis[2-(diphenylphosphino)phenyl] ether oxide) (DPEPO) film, respectively. These emitters also showed high PLQY of 1.00 and 0.87 and small  $\Delta E_{ST}$  of 0.058 and 0.062 eV in the doped film state, respectively. The OLED devices showed maximum EQE and the Commission Internationale de l'Éclairage (CIE) color coordinates of 21.6% and (0.18, 0.43) for **2DAC-Mes3B** and 14.0% as well as (0.17, 0.30) for **DAC-Mes3B**. Additionally, Kitamoto et al. (2016) reported another dimesitylarylborane-based blue TADF emitters. They attached carbazole and 9,9-dimethylacridane moieties as electron-donating units (Kitamoto et al., 2016). Both emitters showed blue emission in the toluene solution; however, carbazole-based emitter exhibited a large  $\Delta E_{ST}$  of 0.456 eV and no TADF characteristics. The  $\Delta E_{ST}$  and PLQY of **9,9-dimethyl-10-(4-(dimesitylboryl)phenyl)-9,10-dihydroacridine (DMBP-Ac)** were shown to be 0.041 eV and 0.83 in 6 wt% doped 1,3-Bis(N-carbazolyl)benzene (mCP) film. The OLED device exhibited a maximum EQE of 16.0% and the CIE color coordinates of (0.14, 0.24). They successfully demonstrated the promising potential of organoboron compounds as highly efficient blue TADF emitters. In 2017, Lee et al. (2017) reported triarylboron TADF emitters coupled with the donor in *ortho* and *para* positions. *Ortho*-positioned donor-acceptor skeleton possessed small enough  $\Delta E_{ST}$  to have a good TADF performance, but *para*-positioned emitters had relatively large  $\Delta E_{ST}$ , which was around 0.40 eV. Among *ortho*-positioned emitters, **CzoB** showed a blue emission peak at 466 nm, high PLQY of 0.84, and a small  $\Delta E_{ST}$  of 0.124 eV in 20 wt% of doped DPEPO film. The OLED device showed a maximum EQE of 22.6% (or 24.1%) and CIE color coordinates of (0.139, 0.150) or (0.139, 0.198) depending on the thickness of indium tin oxide (ITO). They showed that spatially hindered *ortho* donor-acceptor skeleton is effective for achieving small  $\Delta E_{ST}$  and efficient TADF emitter. Later, the same group enhanced the TADF device performance and emission color by manipulating the electronic structure (Lee et al., 2018). They synthesized a series of donor-acceptor-type emitters based on **CzoB (BuCzoB, BuCzMeoB, CzMeoB, and CzOMeOB)** by introducing substituents into the donor and/or acceptor. They inserted tert-Bu, Me, and OMe into carbazole donor and/or to the phenyl ring of the acceptor. These four emitters showed maximum blue emission peak at 485, 478, 456, and 445 nm in 10–20 wt% doped DPEPO film, respectively. The corresponding PLQYs were 0.91, 0.93, 0.83, and 0.63 and small  $\Delta E_{ST}$  values from 0.084 to 0.14 eV, respectively. The fabricated TADF devices exhibited electroluminescence peak from deep blue to sky blue and high EQE. **BuCzoB** showed a maximum EQE of 26.1% and CIE of (0.142, 0.344). Also, the **BuCzMeoB** device showed the highest EQE of 32.8% and CIE of (0.135, 0.266). On the other hand, **CzMeoB**- and **CzOMeOB**-based devices showed a maximum EQE of 18.4 and 17.3% and deep blue color coordinates of (0.138, 0.140) and (0.150, 0.086), respectively. This study showed that the *ortho*-carbazole triarylboron compounds can satisfy the high efficiency of blue TADF emitters. Also, by using substituents to donor and/or acceptor position of CzoB backbone molecule, color and efficiency can be adjusted

successfully. Triarylboron-based blue TADF emitters are listed in **Figure 2** and **Table 1**.

## Partially Bridged Boron-Type Acceptor for Blue Thermally Activated Delayed Fluorescence Emitters

In 2015, Kitamoto et al. (2015) designed boron-incorporated aromatic moiety into the  $\pi$ -conjugated system. Unlike prior triarylboron compounds, they inserted the boron atom into the closed ring system and connected the phenyl linker and donor in the *para* position. They reported 10H-phenoxaborin acceptor-based blue TADF emitters containing carbazole and 9,9-dimethylacridine donors (Kitamoto et al., 2015). They connected 10H-phenoxaborin acceptor and these donors through a phenyl linker at the 1,4 positions. Therefore, quasi anthracene and fluorine units would have a large dihedral angle between hydrogen atoms of phenyl linker, donor, and boron acceptor, resulting in a small overlap of HOMO and LUMO and small  $\Delta E_{ST}$  value. Both molecules showed blue emission in the toluene solution. Even though carbazole-based emitter exhibited deep blue emission, due to the large  $\Delta E_{ST}$  of 0.35 eV, it had no delayed fluorescence component. However, **9,9-dimethyl-10-(4-(10H-phenoxaborin)phenyl)-9,10-dihydroacridine (DBOP-Ac)** had a small  $\Delta E_{ST}$  of 0.013 eV and high PLQY of 0.98 in 6 wt% doped DPEPO film. The device showed maximum EQE of 15.1% and EL spectrum peak at 466 nm, indicating that the boron-based acceptor can be promising candidates for developing blue TADF emitter. Meanwhile, Numata et al. (2015) reported four types of blue TADF emitters based on 10H-phenoxaborin acceptor and acridan donor units. Using the electron-withdrawing property of boron atom, bulky 2,4,6-triisopropylphenyl (TIPP) unit was directly substituted to boron atom so that it can protect the boron atom against the nucleophilic species such as oxygen and water. In addition, acridan donors and 1,3,6,8-tetramethyl-carbazole were selected as the donor moieties due to their good electron-donating property and expectation of large dihedral angle between acceptor arising from the hydrogen atom. Therefore, they synthesized **9,9-dimethyl-10-(10-(2,4,6-triisopropylphenyl)-10H-dibenzo[b,e][1,4]oxaborinin-3-yl)-9,10-dihydroacridine (PXB-Ac)**, **10-(10-(2,4,6-triisopropylphenyl)-10H-dibenzo[b,e][1,4]oxaborinin-3-yl)-10Hspiro[acridine-9,9'-fluorene] (PXB-SAc)**, **10-(10-(2,4,6-triisopropylphenyl)-10H-dibenzo[b,e][1,4]oxaborinin-3-yl)-10Hspiro[acridine-9,9'-xanthene] (PXB-SAcO)**, and **1,3,6,8-tetramethyl-9-(10-(2,4,6-triisopropylphenyl)-10Hdibenzo[b,e][1,4]oxaborinin-3-yl)-9H-carbazole (PXB-TMCz)**. As expected, all emitters exhibited a small  $\Delta E_{ST}$  of around 0.06–0.12 eV, confirming TADF characteristics. All emitters showed blue emission in toluene solution and maximum PL peaks at 475, 456, 451, and 443 nm and high PLQY of 1.00, 0.76, 0.56, and 0.86 for emitters 1–4, respectively, in 20 wt% doped 2,8-bis(diphenylphosphineoxide)dibenzofuran (PPF) film. The OLED devices based on the TADF emitters (**PXB-Ac**, **PXB-SAc**, **PXB-SAcO**, and **PXB-TMCz**) exhibited high EQE of 21.7, 19.0, 20.1, and 13.3%, respectively, and blue emission. Especially, CIE color coordinates of **PXB-SAcO** and

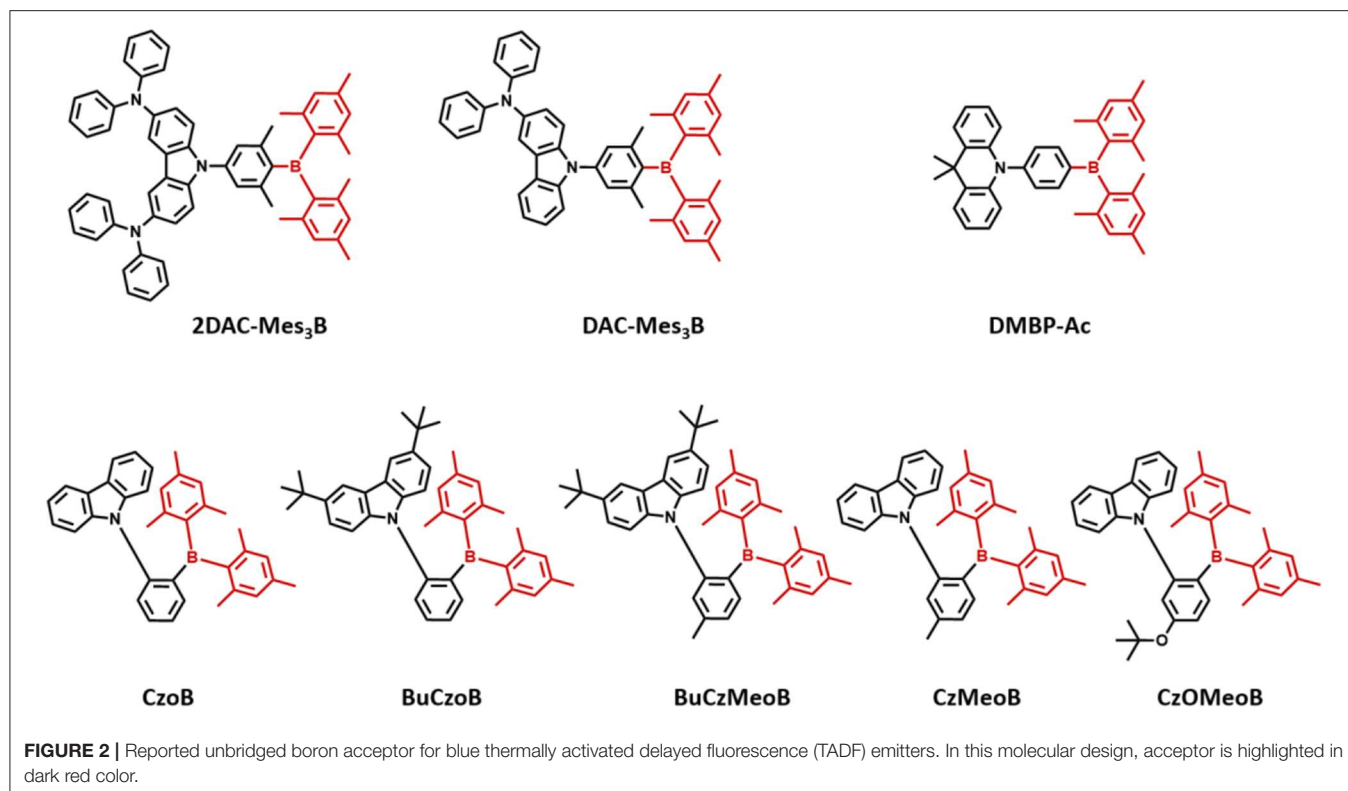


**TABLE 1** | Summary of photophysical properties and device performance of the unbridged boron-type acceptor for blue thermally activated delayed fluorescence (TADF) emitters.

Emitter	$\lambda_{\max}$ [nm]	PLQY	$\Delta E_{ST}^d$ [eV]	$\tau_d$ $\mu$ s	Host	$EQE_{\max}$ [%]	$CE_{\max}$ [ $cdA^{-1}$ ]	CIE 1931 (x, y)	References
2DAC-Mes3B	495 <sup>a</sup>	1.00	0.058	–	DPEPO (16 wt%)	21.6	–	(0.18, 0.43)	Suzuki et al., 2015
DAC-Mes3B	477 <sup>a</sup>	0.87	0.062	–	DPEPO (16 wt%)	14.0	–	(0.17, 0.30)	Suzuki et al., 2015
DMBP-Ac	–	0.83	0.041	6.71 <sup>a</sup>	mCP (6 wt%)	16.0	–	(0.14, 0.24)	Kitamoto et al., 2016
CzoB	466 <sup>c</sup>	0.84	0.124	56.3	DPEPO (20 wt%)	22.6	28.5	(0.139, 0.150)	Lee et al., 2017
BuCzoB	485 <sup>b</sup>	0.91	0.084	23.0	DPEPO (10 wt%)	26.1	56.9	(0.142, 0.344)	Lee et al., 2018
BuCzMeoB	478 <sup>c</sup>	0.93	0.092	26.6	DPEPO (20 wt%)	32.8	56.8	(0.135, 0.266)	Lee et al., 2018
CzMeoB	456 <sup>c</sup>	0.83	0.13	76.3	DPEPO (20 wt%)	18.4	20.4	(0.138, 0.140)	Lee et al., 2018
CzOMeOB	445 <sup>c</sup>	0.63	0.14	87.3	DPEPO (20 wt%)	17.3	13.1	(0.150, 0.086)	Lee et al., 2018

<sup>a</sup> Measured in oxygen-free toluene solution ( $10^{-5}$  M).

<sup>b</sup> Measured in 10 wt% doped film in DPEPO host.

<sup>c</sup> Measured in 20 wt% doped film in DPEPO host.

<sup>d</sup>  $\Delta E_{ST} = S_1 - T_1$ .

PXB-TMCz were (0.14, 0.16). Later, the same group reported phenazineborin-based blue TADF emitter by using spiroacridan donor, **MFAc-AzB** (Park et al., 2016). For blue emission wavelength, they inserted a phenyl-substituted amino unit in phenazaborin acceptor to weaken the electron-withdrawing

ability of the boron atom. Therefore, their synthesized **MFAc-AzB** material showed a blue emission peak at 467 nm in 20 wt% doped PPF film. Moreover, **MFAc-AzB** exhibited a small  $\Delta E_{ST}$  value of 0.24 eV and PLQY value of 0.99 in 20 wt% doped PPF film and even 0.53 in the neat film state. The **MFAc-AzB**

device showed a maximum EQE of 18.2% and CIE coordinates of (0.15, 0.23). Both studies demonstrated the suitability of 10H-phenoxaborin or phenazineborin compounds for highly efficient blue emission TADF materials. Later, Park et al. (2018) studied a series of dibenzoheteraborin-based blue TADF emitters. They designed a boron center and adjustable bridging heteroatoms, such as sulfur, oxygen, or nitrogen and connected to the dimethyl-diphenylacridan (MPAc) donor. Among them, oxygen-containing **MPAc-Bo** and nitrogen-containing **MPAc-BN** emitters showed blue emission in devices. They exhibited emission peak at 483 and 465 nm and a small  $\Delta E_{ST}$  of 0.024 and 0.05 eV in 50 wt% doped PPF film for MPAc-Bo and MPAc-BN. Moreover, these emitters showed high PLQY values of 0.99 and 0.75 in the same film condition. In the device, **MPAc-Bo** and **MPAc-BN** exhibited sky-blue emission and corresponding CIE color coordinates of (0.16, 0.38) and (0.14, 0.23). The **MPAc-Bo**- and **MPAc-BN**-based devices exhibited maximum EQE of 24.9 and 16.0%, respectively. They developed highly efficient blue TADF emitters utilizing dibenzoheteraborin acceptors such as phenoxaborin and phenazaborin and donor diphenylacridan (MPAc). In 2019, Ahn et al. (2019b) reported two highly efficient blue TADF emitters by using the 10H-phenoxaborin acceptor and two types of indolocarbazole derivative donors, **PXB-mIC** and **PXB-DI**. Due to the weak electron-donating ability of simple carbazole, they introduced carbazole derivative donors such as indolocarbazole and diindolocarbazole (DI). The large electron planes of donors delivered large spatial HOMO volume, leading to high oscillator strength and high PLQY. Also, *meta*-positioned indole moiety caused high steric hindrance between the acceptor and donor, which results in small  $\Delta E_{ST}$  and good TADF performance. The **PXB-DI** and **PXB-mIC** showed blue emission in the toluene solution (emission peak at 458 and 438 nm) and a small  $\Delta E_{ST}$  of 0.09 and 0.19 eV, respectively. Moreover, **PXB-DI** showed a high PLQY of about 0.971 in 20% doped bis(diphenylphosphine oxide)dibenzofuran (DBFPO) film. On the other hand, **PXB-mIC** showed PLQY of 0.631 in the same conditions. Interestingly, **PXB-DI** device exhibited a maximum EQE of 37.4% and CIE color coordinates of (0.16, 0.34). Also, **PXB-mIC** device exhibited a maximum EQE of 18.8% and CIE color coordinates of (0.14, 0.18). Especially, **PXB-mIC** exhibited national television system committee (NTSC) blue characteristic of (0.14, 0.08) and 12.5% of maximum EQE in 5-(5-(2,4,6-triisopropylphenyl)pyridin-2-yl)-5H-benzo[d]benzo[4,5]imidazo[1,2-a]imidazole (PPBI) host (**Figure 3**).

Later, Agou et al. (2020) reported the pentacyclic ladder-heteraborin blue TADF emitters. Many researchers have investigated the boron-containing  $\pi$ -electron system because of its fascinating properties in terms of TADF emitter. Agou et al. (2006, 2007a,b) reported  $\pi$ -extended ladder-type heteraborins, and they showed novel  $\pi$ -extended ladder-type blue TADF emitters, **MCz-BOBO** and **MCz-BSBS**, by using oxaborin and thiaborin acceptor and MCz donor units, respectively. The **MCz-BOBO** showed a PL emission peak at 476 nm in 20 wt% doped PPF film and a small  $\Delta E_{ST}$  of 0.01 eV. However, **MCz-BSBS** showed a slightly red-shifted emission peak at 483 nm and  $\Delta E_{ST}$  of 0.17 eV. Both emitters exhibited high PLQY values of

1.0 and 0.93, respectively. The **MCz-BOBO** device exhibited maximum EQE of 20.1% and CIE color coordinates of (0.13, 0.20). Also, **MCz-BSBS** showed a maximum EQE of 25.9% and CIE color coordinates of (0.14, 0.33). Both  $\pi$ -extended heteraborins and multi heteroatoms-based materials successively demonstrated excellent blue TADF performance and suggested the development of highly efficient blue TADF emitters.

In 2019, Matsuo and Yasuda (2019) reported boronate- and borinate-based blue TADF emitters. To accomplish a wider energy gap for blue emission wavelength, they examined boronated and borinated esters. They expected that nearby oxygen atoms can donate electrons and diminish the electron deficiency of the boron atom and decrease the electron-withdrawing ability of boron acceptors. The superiority of borinate- and boronate-containing TADF emitters has not been elucidated yet. Therefore, they synthesized two types of boronate TADF emitter, **10-(8,9-dioxa-8a-borabenzofluorene-2-yl)-2,7-dimethyl-10H-spiro[acridine-9,9'-fluorene]** (**DOB-MSAc**) and **10-(8,9-dithia-8a-borabenzofluorene-2-yl)-2,7-dimethyl-10H-spiro[acridine-9,9'-fluorene]** (**DSB-MSAc**), and one borinate-based TADF emitter, **2,7-dimethyl-10-(6-(2,4,6-triisopropylphenyl)-6H-dibenzo[c,e][1,2]oxaborinin-9-yl)-10H-spiro[acridine-9,9'-fluorene]** (**OB-MSAc**), using spiro[2,7-dimethylacridan-9,9'-fluorene] as a donor moiety. Boronate-based TADF emitters **DOB-MSAc** and **OB-MSAc** showed PL peaks at 462 and 448 nm in toluene solution, which was significantly blue-shifted compared to that of phenoxaborin-based TADF emitter **MPAc-BO** (477 nm). However, boronate-thioester-based emitter (**DSB-MSAc**) showed a PL peak at 483 nm, and this was slightly blue-shifted compared to the **MPAc-BS** (493 nm). These results are attributed to the decreased electron-accepting ability by replacing of the B-C bond with B-O or B-S bond. Their PLQY and PL peak values in 20 wt% doped PPF films were 0.28, 0.81, and 0.53, and 470, 491, and 458 nm, respectively. They also had a small  $\Delta E_{ST}$  of 0.30, 0.12, and 0.06 eV for **DOB-MSAc**, **DSB-MSAc**, and **OB-MSAc**, respectively. In devices, **DOB-MSAc** and **OB-MSAc** exhibited the maximum EQE (CIE color coordinates) of 5.2% (0.16, 0.22) and 12.8% (0.15, 0.15), respectively. Especially, **DSB-MSAc** showed the highest maximum EQE of 20.9% and CIE color coordinates of (0.17, 0.39) due to its high PLQY. They demonstrated a new molecular design for blue TADF by changing heteroatoms directly connected to the boron atom. The abovementioned partially bridged boron blue TADF emitters are listed in **Figure 4** and **Table 2**.

Later, Li P. et al. (2019) reported a new class of four-coordinate fluoroboron acceptor TADF emitters for the first time. They supposed that susceptible cleavage of B-C bond and vacant p-orbital on central boron atom can be the critical reason for short device lifetime. Therefore, they designed four-coordinate boron-centered tridentate 2,2'-(pyridine-2,6-diyl) diphenolate (dppy) ligand, which is O $\wedge$ N $\wedge$ O type of chelate anticipating better chemical and thermal stabilities. They employed 3,6-di-tert-butylcarbazole (DTC) as an electron donor moiety. **DTC-Ph(dppy)BF** showed the blue emission peak at 468 nm and a small  $\Delta E_{ST}$  of 0.27 eV in the toluene solution. Also, the PLQY value was 0.71 in 5 wt% doped of mCP film. Due to the relatively

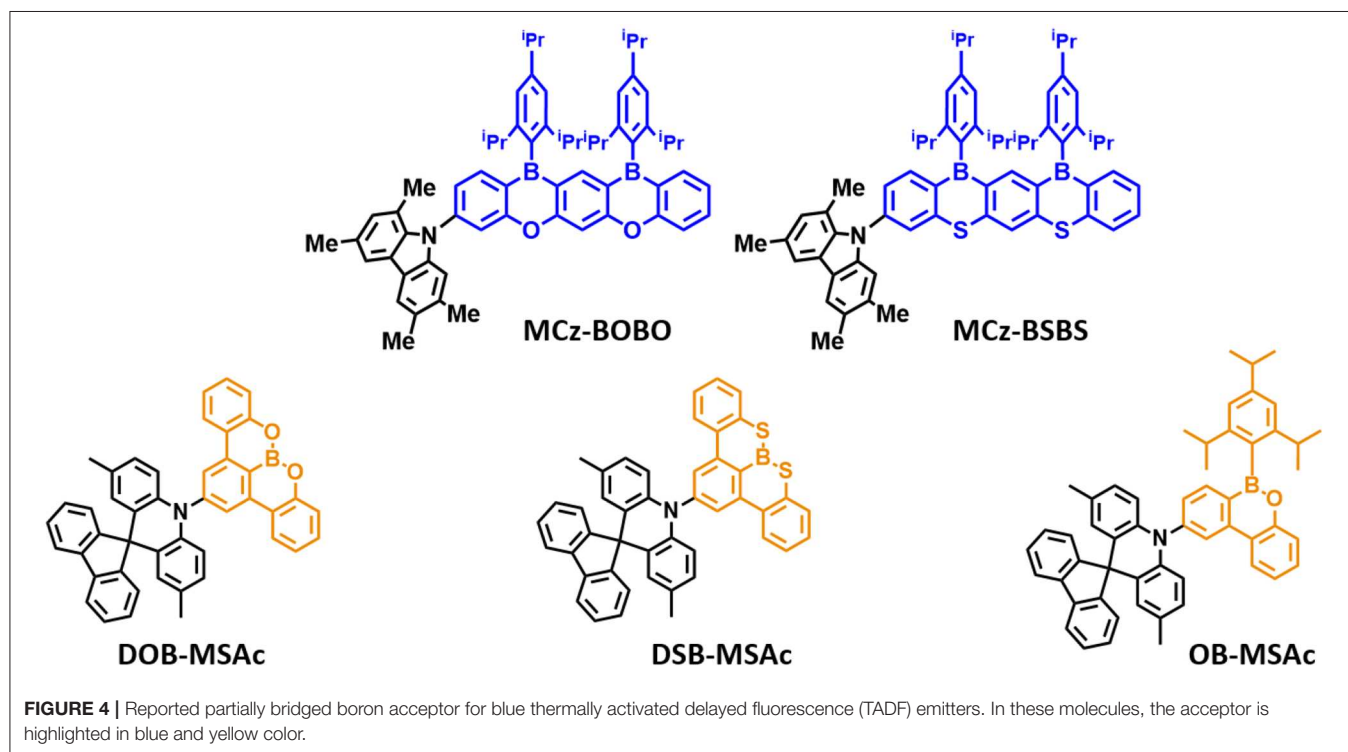
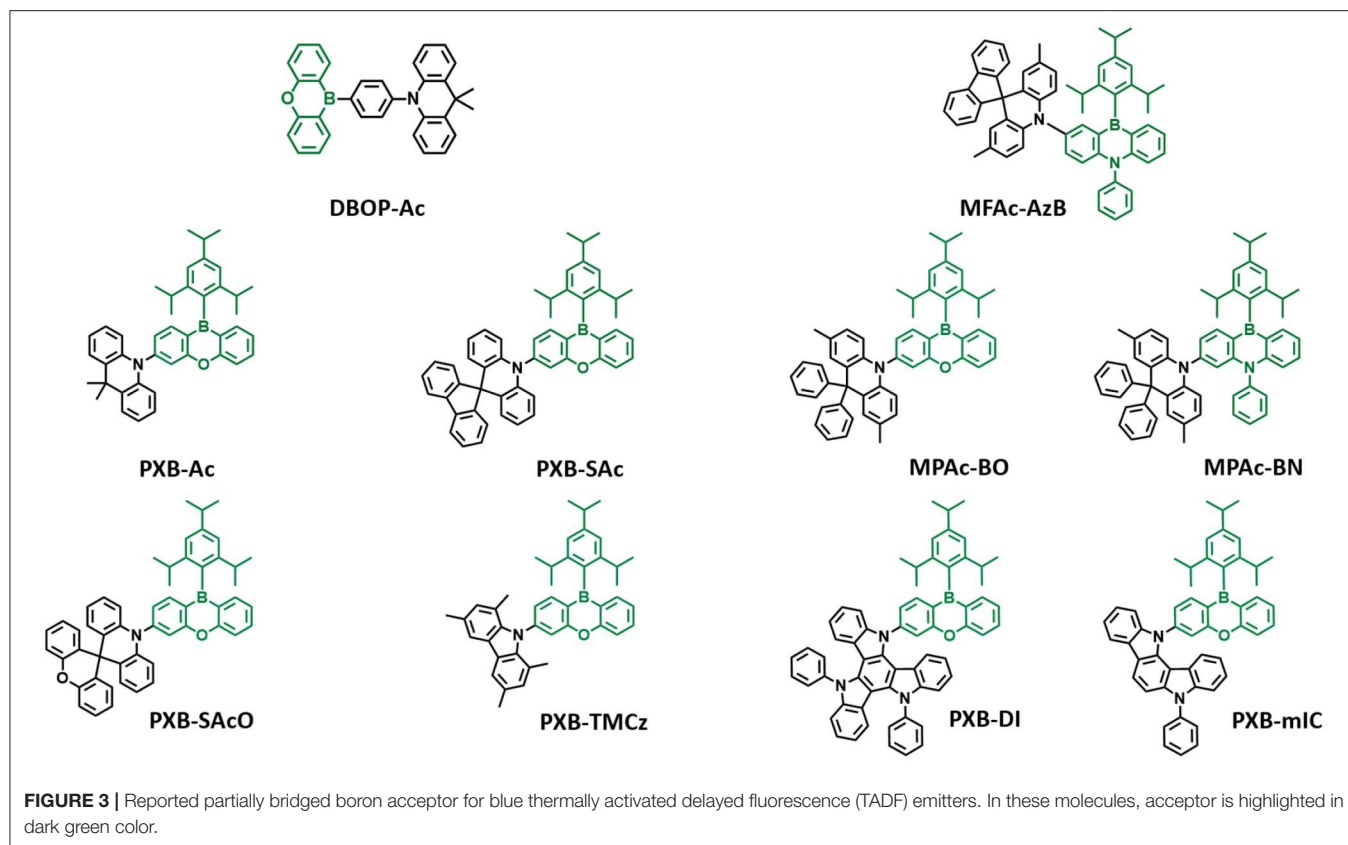


**TABLE 2** | Summary of photophysical properties and device performance of the partially bridged boron-based type blue thermally activated delayed fluorescence (TADF) emitters.

Emitter	$\lambda_{\max}$ [nm]	PLQY	$\Delta E_{ST}^d$ [eV]	$\tau_d$ $\mu\text{s}$	Host	$\text{EQE}_{\max}$ [%]	$\text{CE}_{\max}$ [ $\text{cdA}^{-1}$ ]	CIE 1931 (x, y)	References
DBOP-Ac	–	0.98	0.013	–	DPEPO (6 wt%)	15.1	–	–	Kitamoto et al., 2015
PXB-Ac	475 <sup>a</sup>	1.00	0.10	1.60 <sup>a</sup>	PPF (50 wt%)	21.7	–	–	Numata et al., 2015
PXB-Sac	456 <sup>a</sup>	0.76	0.12	4.02 <sup>a</sup>	PPF (20 wt%)	19.0	–	–	Numata et al., 2015
PXB-SAcO	451 <sup>a</sup>	0.56	0.06	2.06 <sup>a</sup>	PPF (20 wt%)	20.1	–	(0.14, 0.16)	Numata et al., 2015
PXB-TMCz	443 <sup>a</sup>	0.86	0.12	3.49 <sup>a</sup>	PPF (20 wt%)	13.3	–	(0.14, 0.16)	Numata et al., 2015
MFAc-AzB	467 <sup>c</sup>	0.99	0.24	91 PPF (20 wt%)	PPF (20 wt%)	18.2	32.6	(0.15, 0.23)	Park et al., 2016
MPAc-BO	483 <sup>b</sup>	0.99	0.024	1.8 PPF(50 wt%)	PPF (50 wt%)	24.9	57.0	(0.16, 0.38)	Park et al., 2018
MPAc-BN	465 <sup>b</sup>	0.75	0.05	18 PPF (50 wt%)	PPF (50 wt%)	16.0	23.7	(0.14, 0.23)	Park et al., 2018
PXB-mIC	438 <sup>a</sup>	0.631	0.19	3.89/4.04 DBFPO/PPBI (20 wt%)	DBFPO/PPBI (20 wt%)	18.8/12.5	22.1/8.6	(0.14, 0.18)/ (0.14, 0.08)	Ahn et al., 2019b
PXB-DI	458 <sup>a</sup>	0.971	0.09	2.57/3.33 DBFPO/PPBI (20 wt%)	DBFPO/PPBI (20 wt%)	37.4/28.4	66.2/37.8	(0.16, 0.34)/ (0.14, 0.20)	Ahn et al., 2019b
MCz-BOBO	476 <sup>c</sup>	1.00	0.01	0.78 PPF (20 wt%)	PPF (20 wt%)	20.1	31.5	(0.13, 0.20)	Agou et al., 2020
MCz-BSBS	483 <sup>c</sup>	0.93	0.17	2.7 PPF (20 wt%)	PPF (20 wt%)	25.9	52.9	(0.14, 0.33)	Agou et al., 2020
DOB-MSAc	470 <sup>c</sup>	0.28	0.30	140 PPF (20 wt%)	PPF (20 wt%)	5.2	–	(0.16, 0.22)	Matsuo and Yasuda, 2019
DSB-MSAc	491 <sup>c</sup>	0.81	0.12	22 PPF (20 wt%)	PPF (20 wt%)	20.9	–	(0.17, 0.39)	Matsuo and Yasuda, 2019
OB-MSAc	458 <sup>c</sup>	0.53	0.06	12 PPF (20 wt%)	PPF (20 wt%)	12.8	–	(0.15, 0.15)	Matsuo and Yasuda, 2019

<sup>a</sup> Measured in oxygen-free toluene solution ( $10^{-5}$  M).

<sup>b</sup> Measured in 50 wt% doped film in PPF host.

<sup>c</sup> Measured in 20 wt% doped film in PPF host.

<sup>d</sup>  $\Delta E_{ST} = S_1 - T_1$ .

large  $\Delta E_{ST}$  value, RISC efficiency was limited, and maximum EQE was up to 8.8% and CIE color coordinates of (0.16, 0.31). However, the half-lifetime at a constant driving current density of 10 mA/cm<sup>2</sup> reached to 2,354 h. They demonstrated the first trial of design and synthesis of four-coordinate boron and tridentate dppy ligand-based blue TADF emitters. Later, Li G. et al. (2019) reported a new series of tetracoordinated blue TADF emitters using donor–acceptor BF<sub>2</sub>-type skeleton. Tetracoordinated difluoroboron molecules are air-stable, and they can enhance the molecular rigidity to have a high PLQY. They synthesized a series of BF<sub>2</sub>-type acceptor using different donors, especially **NOBF<sub>2</sub>-Cz**, **NOBF<sub>2</sub>-DTCz**, **NOBF<sub>2</sub>-DPCz**, and **NOBF<sub>2</sub>-DMAC**. Except for **NOBF<sub>2</sub>-DMAC**, the other three emitters showed blue emission in the toluene solution from 449 to 473 nm and a small  $\Delta E_{ST}$  of around 0.20 eV. The PLQY values of **NOBF<sub>2</sub>-Cz**, **NOBF<sub>2</sub>-DTCz**, and **NOBF<sub>2</sub>-DPCz** in 10 wt% doped DPEPO film were 0.99, 0.74, 0.70, respectively. In device, they showed the maximum EQE and CIE color coordinates of 11.0% and (0.14, 0.16) for **NOBF<sub>2</sub>-Cz**, 12.7% and (0.14, 0.21) for **NOBF<sub>2</sub>-DTCz**, and 15.8% and (0.14, 0.28) for **NOBF<sub>2</sub>-DPCz**. They demonstrated that tetracoordinated difluoroboron-based

materials can act as stable and efficient TADF emitters (**Figure 5** and **Table 3**).

Three-coordinate organoborane compounds successfully act as electron acceptors in the blue TADF, and in most cases, reactive boron center is surrounded by sterically bulky 2,4,6-trimethylphenyl (Mes) groups. Although these bulky aryl groups protect the center boron from hydrolysis and unstable conditions, highly steric moieties disturb intermolecular interaction and cause detrimental results in solid-state performance. And the sole boron atom itself was not enough to satisfy the deep blue emission. Therefore, researchers searched the alternative strategy not only stabilizes the boron but also tunes deeper blue emission, so that they inserted the boron atom in  $\pi$ -conjugated system with heteroatoms. This strategy enables us to have a structurally constraint skeleton, good molecular rigidity, and intermolecular interaction in solid state. Secondly, by introducing the heteroatom, better TADF properties and pure blue color were achieved, demonstrating partially bridged boron-based TADF more sufficiently satisfied the requirement of blue material.

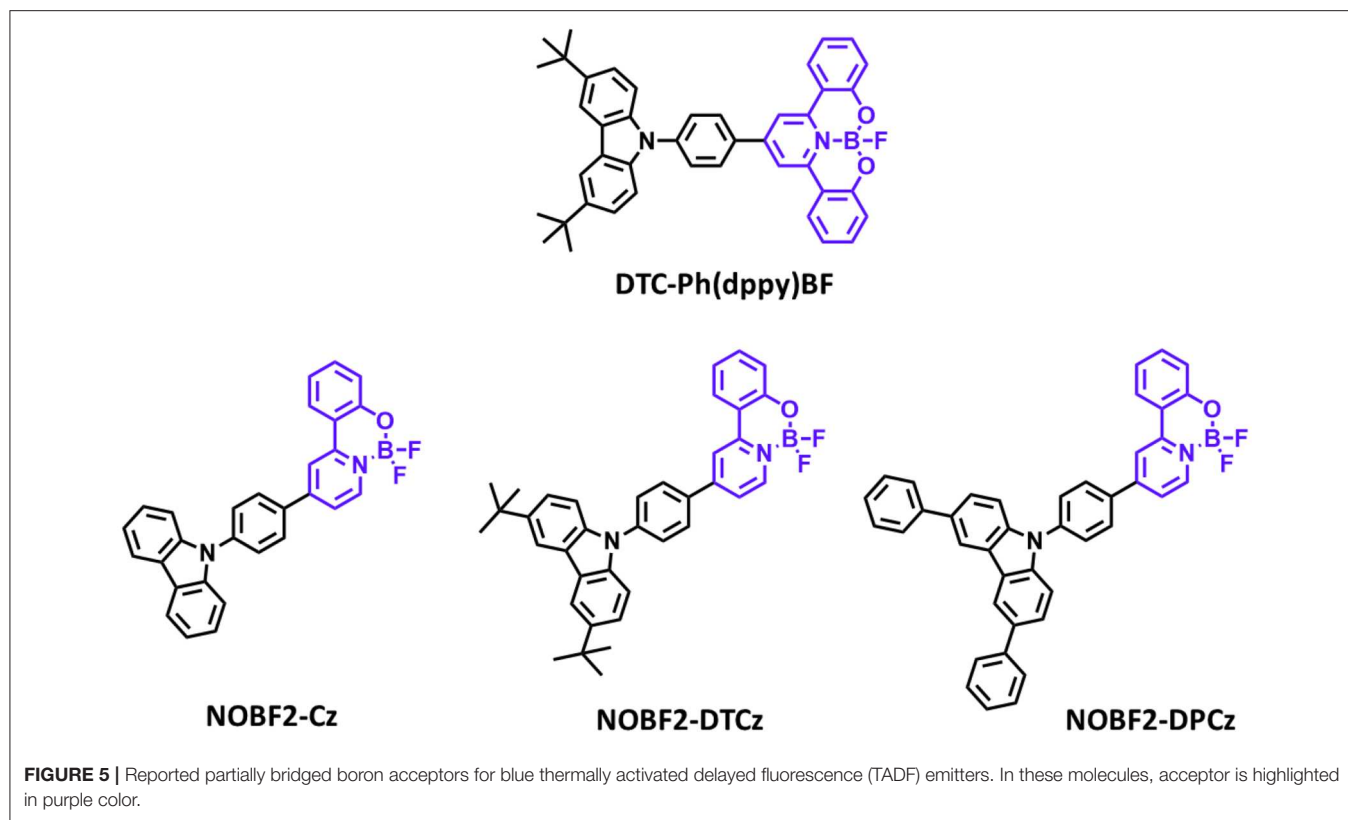


**TABLE 3** | Summary of photophysical properties and device performance of the tetracoordinated difluoroboron-based blue thermally activated fluorescence (TADF) emitters.

Emitter	$\lambda_{\max}$ [nm]	PLQY	$\Delta E_{ST}$ <sup>b</sup> [eV]	$\tau_d$ $\mu$ s	Host	$EQE_{\max}$ [%]	$CE_{\max}$ [cdA <sup>-1</sup> ]	CIE 1931 (x, y)	References
DTC-Ph(dppy)BF	468 <sup>a</sup>	0.71	0.27	–	mCBP (14 wt%)	8.8	17.9	(0.16, 0.31)	Li P. et al., 2019
NOBF2-Cz	449 <sup>a</sup>	0.99	0.20	132	mCBP DPEPO (10 wt%) (10 wt%)	11.0	12.6	(0.14, 0.16)	Li G. et al., 2019
NOBF2-DTCz	473 <sup>a</sup>	0.74	0.20	126	mCBP DPEPO (10 wt%) (10 wt%)	12.7	40.6	(0.14, 0.21)	Li G. et al., 2019
NOBF2-DPCz	471 <sup>a</sup>	0.70	0.22	110	mCBP DPEPO (10 wt%) (10 wt%)	15.8	25.3	(0.14, 0.28)	Li G. et al., 2019

<sup>a</sup>Measured in oxygen-free toluene solution ( $10^{-5}$  M).

<sup>b</sup> $\Delta E_{ST} = S_1 - T_1$ .

## Oxygen-Based Fully Bridged Boron-Type Acceptor for Blue Thermally Activated Delayed Fluorescence Emitters

Recently, triarylboron-based acceptors consisting bridged cyclized unit in donor–acceptor structure have reported good blue TADF performance. Normally, both nitrogen- or oxygen-based fully bridged boron-type acceptor-based materials showed deep-blue emission, narrow FWHM, and good TADF performance. Therefore, such acceptor structure can be used for the design of efficient and stable TADF emitters.

Recently, very few oxygen-based fully bridged boron type TADF emitters have reported by attaching a donor unit to

the central phenyl ring of the oxygen-based fully bridged boron unit on the para-position of the boron atom. The initial sky-blue TADF emitter containing oxygen-based fully bridged boron acceptor and phenoxazine donor (**10-(5,9-dioxa-13b-branaphtho[3,2,1-de]anthracene-7-yl)-10H-phenoxazine** (DOBNA-PX) was reported by Hirai et al. (2015) in 2015. Their emitter showed a sky-blue emission (492 nm), absolute PLQY of 0.92 in 1 wt% doped poly(methyl methacrylate) (PMMA) film, and a small  $\Delta E_{ST}$  of 0.06 eV due to the localization of the single occupied molecular orbitals (SOMOs). They showed an EQE of about 13.9% for the DOBNA-PX-based OLED. Though the performances of DOBNA-PX emitters are lower than the

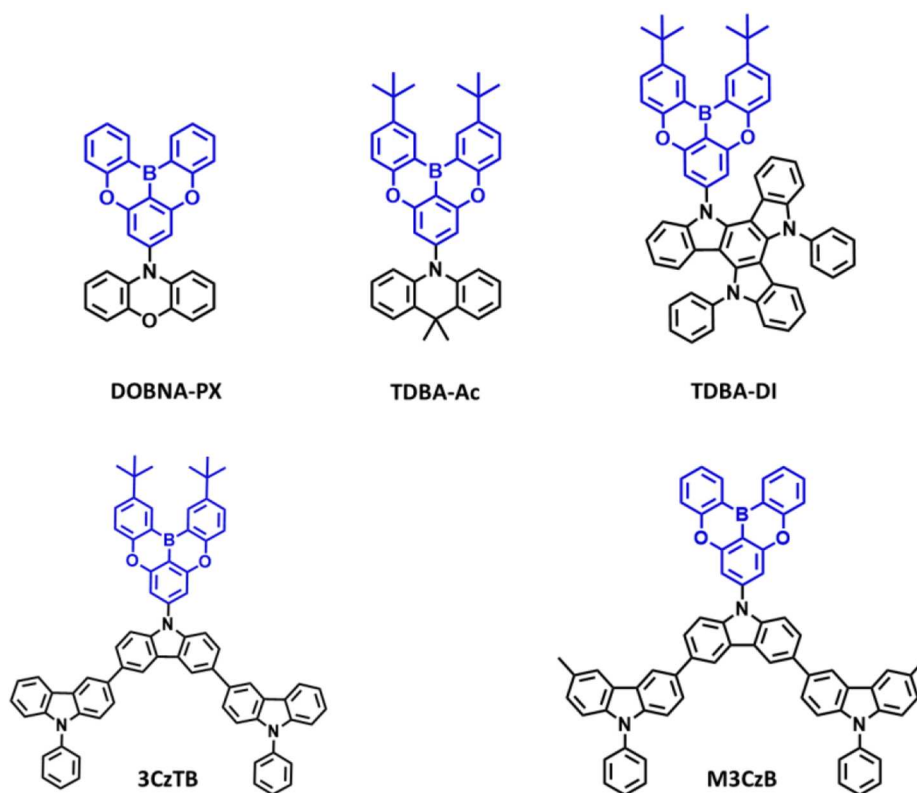


**FIGURE 6** | Reported structures of blue thermally activated delayed fluorescence (TADF) emitters using oxygen-based fully bridged boron acceptor and different donors.

expectation, this study showed the suitable properties of blue TADF emitters. This acceptor moiety can also act as a strong electron acceptor, and it can be suitable to achieve horizontal molecular orientation because of its rigid and symmetrical configuration (Kim and Kim, 2018).

Secondly, in 2019, Ahn et al. (2019a) reported two new highly efficient blue TADF emitters, **TDBA-Ac** and **TDBA-DI** (Figure 6). To satisfy the requirements of the blue TADF materials, they used oxygen-based fully bridged triarylboron with tert-butyl group on the periphery of terminal phenyl ring as an acceptor and DI or acridine (Ac) as donor in the emitter structure. They found that rigid ring-based DI can be used to achieve a large twist angle with an acceptor (Kim et al., 2018). Both emitters, **TDBA-Ac** and **TDBA-DI**, showed a deep-blue emission and maximum PL peak at 458 and 456 nm, respectively, in solution state. These emitters also exhibited a narrow FWHM of about 50 (**TDBA-Ac**) and 55 nm (**TDBA-DI**). The calculated singlet and triplet energies from the onset of the RTPL and LTPL spectra of **TDBA-Ac** and **TDBA-DI** were 3.11/3.05 and 3.06/2.95 eV, respectively. Both of these emitters exhibited small  $\Delta E_{ST}$  values of 0.06 (in solution state) and 0.05 eV (20 wt% doped **TDBA-DI** in DBFPO film) for **TDBA-Ac** and **TDBA-DI**, respectively. They found a delayed exciton lifetime of 1.82 and 1.79  $\mu\text{s}$  for **TDBA-Ac** and **TDBA-DI**, respectively, which was shorter than the reported blue TADF

emitters. **TDBA-Ac** (20 wt%) and **TDBA-DI** (20 wt%) in the DBFPO host showed a PLQY of 0.93 and 0.99, respectively. Also, the HOMO dispersing molecular design of emitters and low non-radiative decay rates were responsible for achieving high PLQY. The **TDBA-Ac**- and **TDBA-DI**-based OLEDs (DBFPO host) exhibited maximum EQE of 25.71 and 38.15%, respectively. The **TDBA-DI** device showed a maximum luminance of 47,680  $\text{cd}/\text{m}^2$  and a horizontal dipole orientation ratio of 0.89. Such high efficiency, high luminance, and good color coordinates were attributed to the highly conjugated and rigid donor and acceptor combination for high PLQY and narrow emission, the large dihedral angle between the donor and acceptor for small  $\Delta E_{ST}$ , fast RISC, and horizontal molecular orientation. Also, the **TDBA-DI** emitter and mCBP-CN host system device showed an operational lifetime ( $T_{50}$ ) of 55.2 h at the initial luminance of 1,000  $\text{cd}/\text{m}^2$ . They also reported **DBA-DI** emitter by removing tert-butyl from the **TDBA-DI** to achieve high efficiency and long lifetime (Ahn et al., 2020). The **DBA-DI** showed slight variations in the photophysical properties compared to the **TDBA-DI** as shown in Table 4. However, the **DBA-DI** device exhibited high EQE of 26.4%, CIE color coordinates of (0.17, 0.40), and lifetime of 540 h at the initial luminance of 1,000  $\text{cd}/\text{m}^2$ .

Later, they reported a series of blue TADF emitters consisting of oxygen-based fully bridged triarylboron acceptor and tercarbazole donor. These two emitters, **3CzTB** and **M3CzB**,

**TABLE 4** | Summary of photophysical and device characteristics of the oxygen-based fully bridged boron type blue thermally activated delayed fluorescence (TADF) emitters.

Emitter	$\lambda_{\max}$ [nm]	PLQY	$\Delta E_{ST}^d$ [eV]	$\tau_d$ $\mu$ s	Host	$EQE_{\max}$ [%]	$CE_{\max}$ [cdA <sup>-1</sup> ]	CIE 1931 (x, y)	References
DOBNA-PX	492 <sup>c</sup>	0.92	0.06	31.8	CBP (20 wt%)	13.9	40.1	–	Hirai et al., 2015
TDBA-Ac	458 <sup>a</sup>	0.93	0.06	1.82	DBFPO (20 wt%)	25.71	27.73	(0.14, 0.15)	Ahn et al., 2019a
TDBA-DI	456 <sup>a</sup>	0.99	0.05	1.79	DBFPO (20 wt%)	38.15	64.38	(0.15, 0.28)	Ahn et al., 2019a
DBA-DI	467 <sup>a</sup>	95.3	0.03	1.25	mCBP-CN: DDBFT (30 wt%)	26.4	–	(0.17, 0.40)	Ahn et al., 2020
3CzTB	433 <sup>a</sup>	0.87	0.23	9.32	DBFPO (20 wt%)	29.1	36.4	(0.14, 0.19)	Karthik et al., 2020
M3CzB	445 <sup>a</sup>	0.92	0.14	7.84	DBFPO (20 wt%)	30.7	46.7	(0.14, 0.26)	Karthik et al., 2020
OBA-O	444 <sup>a</sup>	0.84	0.09	4.14	mCP (5 wt%)	17.8	33.2	(0.17, 0.17)	Song et al., 2019
OBA-S	456 <sup>a</sup>	0.75	0.09	4.80	mCP (5 wt%)	4.4	6.3	(0.20, 0.31)	Song et al., 2019
OBA-BrO	470 <sup>a</sup>	0.92	0.04	3.74	mCP (5 wt%)	22.5	49.2	(0.21, 0.38)	Song et al., 2019
OBA-BrS	478 <sup>a</sup>	0.55	0.07	0.81	mCP (5 wt%)	9.2	20.3	(0.29, 0.46)	Song et al., 2019
m-AC-DBNA	492 <sup>b</sup>	0.89	0.009	7.6	BCPO (10 wt%)	17.1	42.0	(0.18, 0.42)	Meng et al., 2019
m'-AC-DBNA	498 <sup>b</sup>	0.96	0.031	1.5	BCPO (10 wt%)	14.1	35.3	(0.18, 0.39)	Meng et al., 2019
p-AC-DBNA	496 <sup>b</sup>	0.87	0.009	7.8	BCPO (10 wt%)	20.5	47.4	(0.17, 0.36)	Meng et al., 2019

<sup>a</sup> Measured in toluene solvent.<sup>b</sup> Measured in 10 wt% doped film in BCPO host.<sup>c</sup> Measured in 1 wt% doped film in PMMA host.<sup>d</sup>  $\Delta E_{ST} = S_1 - T_1$ .

were designed by alkyl modification on the donor and acceptor units, which changes not only their donor–acceptor interaction but also the electronic nature (Karthik et al., 2020). 6,6'-Dimethyl substituted tercarbazole moiety was used as a donor unit and attached to the oxygen-based fully bridged triarylboron acceptor (**M3CzB**) to improve the electrochemical stability of the TADF emitter. The tert-butyl-modified boron acceptor has attached to the methyl group-modified tercarbazole donor (**3CzTB**) to tune the acceptor strength. These emitters, **3CzTB** and **M3CzB**, showed emission wavelength and  $\Delta E_{ST}$  of 433 nm and 0.23 eV and 445 nm and 0.14 eV, respectively, in the solution state. Also, **3CzTB** and **M3CzB** showed a delayed exciton lifetime of 9.32 and 7.84  $\mu$ s, respectively, which was measured from the 20 wt% doped DBFPO films. However, **M3CzB** showed a higher RISC rate and lower triplet non-radiative rate compared to the **3CzTB** because of its low  $\Delta E_{ST}$ . The **3CzTB**- and **M3CzB**-based OLEDs exhibited a high EQE of 29.1 and 30.7%, respectively, which was attributed to the high PLQY, fast RISC, and horizontal dipole orientation of the emitter. These devices also showed a maximum luminance of 18,160 cd/m<sup>2</sup> for **M3CzB** and 11,690 cd/m<sup>2</sup> for **3CzTB**.

Recently, several other TADF materials were synthesized by attaching different donor units to the central phenyl ring of the oxygen-based fully bridged boron acceptor (**OBA**) on the meta-position of the boron. Song et al. (2019) reported four new TADF emitters, **OBA-O**, **OBA-S**, **OBA-BrO**, and **OBA-BrS**, by using oxygen-based fully bridged boron acceptors (**OBA** or **DBA**) and phenoxazine or phenothiazine donors (**Figure 7**). Also, they attached Br- group to the **OBA** unit (**OBA-Br**) to improve the TADF properties of the emitter. The phenothiazyl-based emitters showed longer maximum emission wavelengths of 456 (**OBA-S**) and 478 nm (**OBA-BrS**) in the solution state compared to phenoxazyl-based materials (**OBA-O**: 444 nm and **OBA-BrO**: 470 nm) because of stronger donating ability of the phenothiazyl. The blue TADF emitter **OBA-O** and its blue analog **OBA-BrO** showed higher PLQY values of 0.84 and 0.92, respectively, than both **OBA-S** (0.75) and **OBA-BrS** (0.55). All these emitters showed very small  $\Delta E_{ST}$  values <0.1 eV and good TADF properties due to the large twist angle near to 90° between the donor and acceptor, which makes separation of the natural transition orbitals. They achieved  $\Delta E_{ST}$  of 0.09 eV for **OBA-O** and **OBA-S**, while 0.04 and 0.07 eV for **OBA-BrO** and

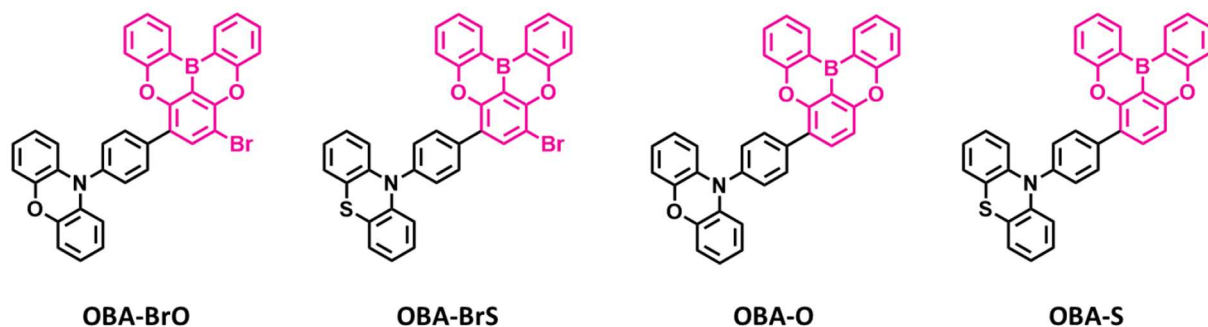


**FIGURE 7** | Reported structures of blue thermally activated delayed fluorescence (TADF) emitters using oxygen-based fully bridged boron acceptor and different donors.

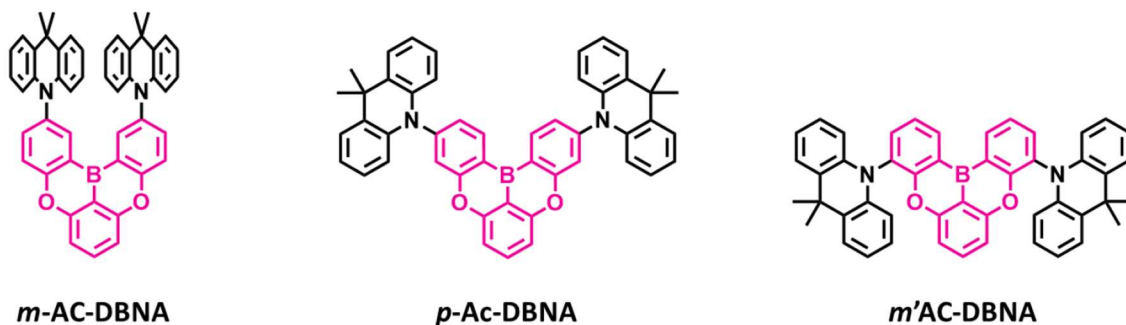


**FIGURE 8** | Reported structures of blue thermally activated delayed fluorescence (TADF) emitters using donor units attached to the different positions of the boron-based acceptor.

**OBA-BrS**, respectively. On the other hand, both -Br-attached TADF emitters showed shorter delayed exciton lifetime (higher  $K_{\text{RISC}}$ ) of 3.74 ( $8.97 \times 10^5 \text{ s}^{-1}$ ) and 0.81  $\mu\text{s}$  ( $8.41 \times 10^5 \text{ s}^{-1}$ ) for **OBA-BrO** and **OBA-BrS**, respectively, compared to **OBA-O** (4.14  $\mu\text{s}$  and  $4.28 \times 10^5 \text{ s}^{-1}$ ) and **OBA-S** (4.80  $\mu\text{s}$  and  $2.76 \times 10^5 \text{ s}^{-1}$ ) due to their smaller  $\Delta E_{\text{ST}}$  values. Such a high  $K_{\text{RISC}}$  was attributed to the electron-withdrawing ability of -Br group on the OBA acceptor that will improve the TADF process in **OBA-BrO** and **OBA-BrS**. **OBA-O** and **OBA-BrO** devices showed higher EQE of 17.8 and 22.5% than **OBA-S** (4.4%) and **OBA-BrS** (9.2%) devices because of their higher PLQY values. Among these TADF materials, **OBA-O** device showed the bluest CIE color coordinates (0.17, 0.17) and a maximum EL peak of 446 nm. However, other emitter-based devices showed sky-blue CIE color coordinates (**Table 4**).

Also, another series of TADF emitters were reported by using donor unit into the different positions of the oxygen-based fully bridged boron acceptor. Meng et al. (2019) reported the effect of substitutional positions of the donor group on the TADF properties of the oxygen-based fully bridged boron-type acceptor-based emitter. They synthesized three different boron-based TADF emitters, **m-AC-DBNA**, **p-AC-DBNA**, and **m'-AC-DBNA**, by using two dimethyl Ac units at meta-, para-, and meta'-positions of the 5,9-dioxa-13b-boranaphtho[3,2,1-de]anthracene (DBNA) (**Figure 8**). They selected Ac as a donor

unit because of its strong electron-donating property and suitable steric hindrance for the TADF molecule. They checked an effect of such molecular design on intermolecular interactions, thermal and photophysical properties, and EL performance. All three emitters showed an emission peak at 514–518-nm range (film state). However, PL properties of 5 wt% emitter doped **BCPO** films showed sky-blue emission, which were blue-shifted by about 20 nm than the neat films. A para isomer showed higher PLQY of 0.96 than m- (0.89) and m'- (0.87) isomers in the doped film. The  $\Delta E_{\text{ST}}$  values of all three emitters were measured to be 9.0 (**m-AC-DBNA**), 9.1 (**p-AC-DBNA**), and 31 (**m'-AC-DBNA**) meV. Among all the three isomers, **p-AC-DBNA** exhibited the highest  $K_{\text{RISC}}$  value of  $1.17 \times 10^6 \text{ s}^{-1}$  and delayed exciton lifetime of 1.5  $\mu\text{s}$ . The OLEDs (10% doped TADF materials) exhibited maximum EQE of 17.1, 14.1, and 20.5% for m-, m'-, and p-isomers, respectively. On the other hand, neat p-isomer device showed an excellent maximum EQE of 14.1%. This result shows the doping concentration-independent characteristic of these TADF emitters. The TADF devices (m-, m'-, and p-isomers) exhibited maximum EL peak at 492–488 nm and sky-blue CIE color coordinates.

The above-described TADF emitters containing oxygen-based fully bridged boron acceptors and different donor units exhibited good TADF properties and high efficiency. Interestingly, among the above-described oxygen-based fully bridged boron-type

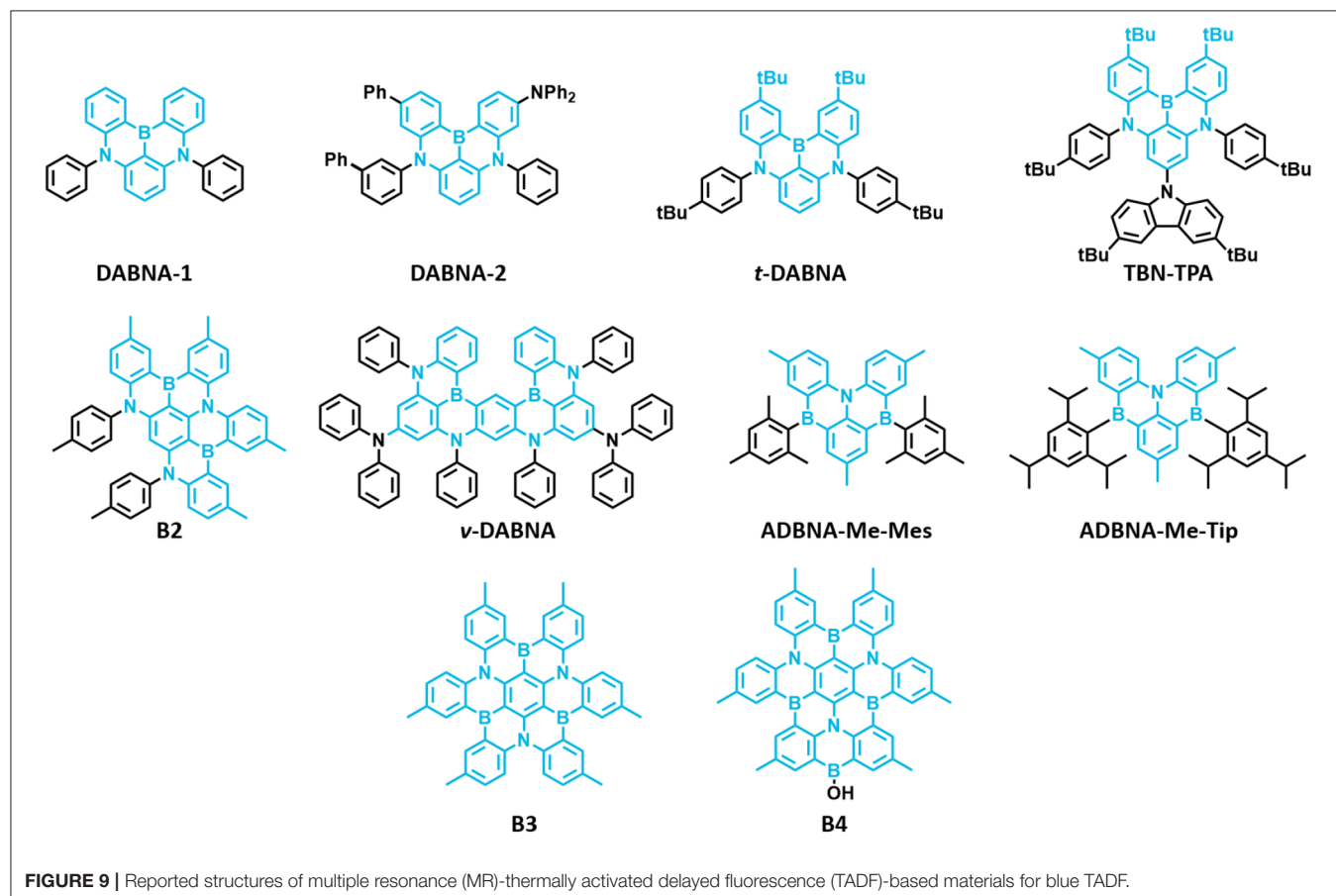
acceptor-based TADF emitters, the design containing donor units attached to the central phenyl ring of the oxygen-based fully bridged boron unit on the *para*-position of the boron atom exhibited excellent TADF and OLED properties.

## Multiple Resonance-Based Structure for Blue Thermally Activated Delayed Fluorescence Emitters

Recently, multiple resonance-TADF (MR-TADF) materials showed good electroluminescence properties due to their high efficiency and color purity. Generally, these materials show very narrow emission profiles because of their rigid and symmetrical structures. Moreover, MR-TADF materials show majorly deep blue emission with high color purity. Unlike the traditional donor-acceptor-type TADF configuration, this type of MR-TADF materials show HOMO and LUMO orbital separation at *ortho* and *para* positions with respect to nitrogen and boron atoms, respectively, within the same conjugated planar core structure. Moreover, this type of materials shows high oscillator strength along with small  $\Delta E_{ST}$ , which is contradictory to conventional TADF materials. Though MR-TADF materials possess several advantages over conventional TADF emitters, they suffer from very limited chemical modification, complicated synthesis, and high-efficiency roll-off. Additionally, the underlying mechanism

behind the high oscillator strength along with small  $\Delta E_{ST}$  is still not clearly known. However, Pershin et al. (2019) studied the insightful mechanism of multiple resonance-based materials by performing Spin-Component Scaling second-order approximate Coupled-Cluster (SCS-CC2) theoretical calculations. The insightful mechanism was predicted by using the wave functions of two metrics such as the electron-hole charge separation distance ( $\Delta r$ ) and the amount of charge transferred ( $\Delta q$ ) between them at the lowest singlet excited state. From there, it was found that a substantial reshuffling of electron density (large  $\Delta q$ ) occurs over short distances (small  $\Delta r$ ), i.e., the “short-range/local CT” state features both high electron-hole wave function overlaps and small exchange interactions resulting in high oscillator strength and small  $\Delta E_{ST}$ , respectively. Further, these behaviors increase as proportional to the increase in molecular conjugation.

The first MR-TADF materials containing one boron atom and two nitrogen atoms, **DABNA-1** and **DABNA-2**, were reported by Hatakeyama et al. (2016) in 2016. These materials exhibited deep blue emission with PLQY and  $\Delta E_{ST}$  of 0.88 and 0.18 eV and 0.90 and 0.15 eV in 1 wt% doped mCBP film for **DABNA-1** and **DABNA-2**, respectively. Also, they showed high EQE values of 13.5% and 20.2% with deep blue color coordinates of (0.13, 0.09) and (0.12, 0.13) along with very narrow EL spectra of FWHM



28 nm for **DABNA-1** and **DABNA-2**, respectively. The high color purity of these materials is attributed to narrow EL spectra with very small FWHM of 28 nm for both materials. Though these materials showed very high efficiency roll-off, they are promising candidates for developing pure deep blue TADF materials. Later, Han et al. (2019) reported the *tert*-butyl-modified **DABNA-1**, **t-DABNA**, which was used with TADF assistant dopant **DMAC-DPS** to increase the device efficiency and to reduce roll-off. This assistant dopant device exhibited improved maximum efficiency from 25.1 to 31.4% and reduced roll-off compared to without assistant dopant device. In another report, **t-DABNA** structure was modified with the addition of carbazole donor on the *para* position to the boron atom to get **TBN-TBA** (Liang et al., 2018). The addition of donor segment gave high PLQY of up to 0.975 and very small  $\Delta E_{ST}$  of 0.03 eV in toluene solution. Also, the blue TADF OLED fabricated with 4 wt% **TBN-TBA** in **2,6-DCzppy** host showed very high EQE of 32.1% with EL maximum of 447 nm and FWHM of 27 nm. Matsui et al. (2018) reported di- and tri-boron doped nanographenes **B2**, **B3**, and **B4** as multiple resonance TADF materials. All materials showed deep blue emission in the range from 441 to 455 nm with small FWHM of 32–34 nm in 1 wt% doped in PMMA films (Matsui et al., 2018). The PLQY values are in the range of 0.33–0.57 and small  $\Delta E_{ST}$  values in the range of 0.15 eV–0.18 eV in PMMA films. The TADF device with **B2** as 1 wt% emitting dopant in mCBP host exhibited maximum EQE of 18.3% with EL peak maximum of 460 nm and FWHM of 37 nm. Later, Kondo et al.

(2019) reported a dimer of **DABNA-1** core, **v-DABNA** with two boron atoms and two diphenylamine donors attached *para* positions to the boron atoms. The photophysical properties of the **v-DABNA** in 1 wt% doped in **DOBNA-OAr** host showed a deep blue emission peak, PLQY, and  $\Delta E_{ST}$  of 467 nm, 0.9, and 17 meV, respectively. Though the conjugation of **v-DABNA** increased doubly compared to **DABNA-1**, the emission peak is retained in the blue region as in **DABNA-1**. But the increase in PLQY and reduction in  $\Delta E_{ST}$  values are observed for **v-DABNA** compared to **DABNA-1**. The TADF device based on **v-DABNA** showed the highest EQE of 34.4% with deep blue CIE coordinates of (0.12, 0.11) with very narrow FWHM of 18 nm. Also, this device showed very low efficiency roll-off of only 8.6% at 1,000 cd/m<sup>2</sup>. This is the highest efficiency of multiple resonance-based TADF materials reported so far. Recently, Nguyen et al. (2020) evaluated the performances of exciplex host-based TADF devices, and they compared the device performances with and without **v-DABNA** as 1 wt% emitting dopant. The maximum EQE and brightness of 8.9% and 830 cd/m<sup>2</sup> and 19% and 1,260 cd/m<sup>2</sup> for the devices with and without **v-DABNA** were observed. Further, the LT<sub>50</sub> lifetime of both devices showed almost similar values (~350 h) and indicates the promising way of making stable devices (Nguyen et al., 2020). Recently, Oda et al. (2019) reported two multiple resonance-based TADF materials, **ADBNA-Me-Mes** and **ADBNA-Me-Tip**; these materials possess one nitrogen atom in the center of the core and two boron atoms in the outer of the core unit. It is interesting to note that

**TABLE 5** | Summary of photophysical properties and device performances of the multiple resonance (MR)-thermally activated delayed fluorescence (TADF)-based blue TADF materials.

Emitter	$\lambda_{\max}$ [nm]	PLQY	$\Delta E_{ST}^e$ [eV]	$\tau_d$ $\mu$ s	Host	EQE <sub>max</sub> [%]	CE <sub>max</sub> [cdA <sup>-1</sup> ]	CIE 1931 (x, y)	References
DABNA-1	460 <sup>a</sup>	0.88	0.18	93.7	mCBP mCBP (1 wt%)	13.5	10.6	(0.13, 0.09)	Hatakeyama et al., 2016
DABNA-2	469 <sup>a</sup>	0.90	0.14	65.3	mCBP mCBP (1 wt%)	20.2	21.1	(0.12, 0.13)	Hatakeyama et al., 2016
B2	455 <sup>b</sup>	0.53	–	30.4	mCBP PMMA (1 wt%)	18.3	16.7	(0.13, 0.11)	Matsui et al., 2018
B3	441 <sup>b</sup>	0.33	–	–	–	–	–	–	Matsui et al., 2018
B4	450 <sup>b</sup>	0.57	–	–	–	–	–	–	Matsui et al., 2018
TBN-TPA	470 <sup>c</sup>	0.97	0.14	51.02	2,6-DCzppy DCzppy (4 wt%)	32.1	40.2	(0.12, 0.19)	Liang et al., 2018
<i>t</i> -DABNA	–	0.85	0.17	83.3	DPEPO DPEPO (-wt%)	25.1	13.0	–	Han et al., 2019
<i>v</i> -DABNA	467 <sup>d</sup>	0.90	0.017	4.1	DOBNA-Oar DOBNA-Oar (1 wt%)	34.4	31.0	(0.12, 0.11)	Kondo et al., 2019
ADBNA-Me-Mes	482 <sup>d</sup>	0.89	0.20	165	DOBNA-Oar DOBNA-Oar (1 wt%)	16.2	15.4 <sup>f</sup>	(0.10, 0.27)	Oda et al., 2019
ADBNA-Me-Tip	479 <sup>d</sup>	0.88	0.19	147	DOBNA-Oar DOBNA-Oar (1 wt%)	21.4	23.5 <sup>f</sup>	(0.11, 0.29)	Oda et al., 2019

<sup>a</sup>Measured in 1 wt% doped film in mCBP host.

<sup>b</sup>Measured in 1 wt% doped film in PMMA host.

<sup>c</sup>Measured in oxygen-free toluene solution ( $5 \times 10^{-5}$  M).

<sup>d</sup>Measured in 1 wt% doped film in DOBNA-OAr host.

<sup>e</sup> $\Delta E_{ST} = S_1 - T_1$ .

<sup>f</sup>Current efficiencies at luminance of maximum, 100 cd/m<sup>2</sup>.

on incorporation of two electron withdrawing boron atoms in the **ADBNA** core, the emission peak is red-shifted about 20 nm compared to **DABNA-1**. Though these two materials showed similar PLQY values compared to **DABNA-1**, they showed little higher  $\Delta E_{ST}$  values than **DABNA-1**. The TADF OLEDs using **ADBNA-Me-Mes** and **ADBNA-Me-Tip** as emitting dopant exhibited sky-blue emission with maximum EQE of 21.4 and 16.2% with little broad emission spectrum (FWHM of 32 and 33 nm), respectively. Apart from blue emission, green multiple resonance-based TADF materials were reported by Zhang et al. (2019) by incorporating weak acceptor groups on the periphery of the **DABNA** core. These results indicate that incorporation of a donor group at the *para* position to boron atom on the **DABNA** core retains the deep blue color, whereas the acceptor group incorporation gives a red-shifted emission color (Figure 9 and Table 5).

Further, it is found that the large conjugated **DABNA**-based material like  $\nu$ -**DABNA** exhibited the highest blue TADF performances due to its small  $\Delta E_{ST}$  and high PLQY. This result reflects the computational prediction by Pershin et al. (*vide supra*). So, the molecular design for the efficient blue MR-TADF should possess either large conjugated molecular structures or attachment of donor at the *para* position to the boron atom of the **DABNA** core.

## CONCLUSIONS AND OUTLOOK

We summarized the boron-containing aromatic acceptor moieties connected with several donors of push-pull small molecules for blue TADF OLED applications. The boron-based TADF materials exhibited good TADF performances with maximum EQE value as high as 38.15%, which is the highest value for blue TADF OLEDs reported so far. We found the order of type of boron-based materials to realize pure blue emission color, high PLQY, small  $\Delta E_{ST}$ , short delayed exciton lifetime, and high efficiency for unbridged < partially bridged < fully bridged boron compounds. Exclusively, the fully bridged oxygen-containing boron acceptor shows an additional property of horizontal dipole orientation which is desirable for highly efficient devices. On the other hand, the fully bridged nitrogen-containing boron materials (MR-TADF) show very

narrow emission in deep blue region. It is concluded that the fully bridged boron compounds would be an ideal candidate for designing highly efficient deep blue TADF materials. Also, attachment of donor at the *para* position to the boron atom of MR-TADF materials would give deep blue color, small  $\Delta E_{ST}$ , high PLQY, and high efficiency. These results indicate that the boron materials are promising for the development of blue TADF OLEDs.

Though the boron-containing materials showed high efficiency, the lifetime of the blue TADF device is still a challenging task. As the delayed exciton lifetime of fully bridged boron materials is short, the usage of them as TADF assistant host for MR-TADF dopant materials in hyperfluorescence devices has advantages of (i) an increase in color purity as emission originates from the MR-TADF dopant, (ii) the dramatically increased device efficiency due to the usage of both host and dopant as TADF materials, and (iii) the increased device lifetime due to the fast Forster resonance energy transfer from the TADF assistant host to the MR-TADF dopant.

## AUTHOR CONTRIBUTIONS

HL, DK, and RL contributed equally to write and revise this manuscript. JR organized all the related tables and figures. JK supervised this work. All authors listed have made a substantial, direct and intellectual contribution to the work, and approved it for publication.

## FUNDING

This work was supported by the National Research Foundation of Korea (Grant No. NRF-2019M3D1A2104019) and the Technology Innovation Program (20006464, Development of TADF sensitized fluorescence RGB emitting layer materials with high color purity and high efficiency for BT 2020) funded by the Ministry of Trade, Industry & Energy (MOTIE, Korea). This work was also supported by Samsung Display Co., Ltd. The funder was not involved in the study design, collection, analysis, interpretation of data, the writing of this article or the decision to submit it for publication.

## REFERENCES

- Agou, T., Kobayashi, J., and Kawashima, T. (2006). Syntheses, structure, and optical properties of ladder-type fused azaborines. *Org. Lett.* 8, 2241–2244. doi: 10.1021/ol060539n
- Agou, T., Kobayashi, J., and Kawashima, T. (2007a). Development of a general route to periphery-functionalized azaborines and ladder-type azaborines by using common intermediates. *Chem. Commun.* 3204–3206. doi: 10.1039/b706418g
- Agou, T., Kobayashi, J., and Kawashima, T. (2007b). Electronic and optical properties of ladder-type heteraborins. *Chem. A Eur. J.* 13, 8051–8060. doi: 10.1002/chem.200700622
- Agou, T., Matsuo, K., Kawano, R., Park, I. S., Hosoya, T., Fukumoto, H., et al. (2020). Pentacyclic ladder-heteraborin emitters exhibiting high-efficiency blue thermally activated delayed fluorescence with an ultrashort emission lifetime. *ACS Mater. Lett.* 2, 28–34. doi: 10.1021/acsmaterialslett.9b00433
- Ahn, D. H., Kim, S. W., Lee, H., Ko, I. J., Karthik, D., Lee, J. Y., et al. (2019a). Highly efficient blue thermally activated delayed fluorescence emitters based on symmetrical and rigid oxygen-bridged boron acceptors. *Nat. Photonics* 13, 540–546. doi: 10.1038/s41566-019-0415-5
- Ahn, D. H., Lee, H., Kim, S. W., Karthik, D., Lee, J., Jeong, H., et al. (2019b). Highly twisted donor-acceptor boron emitter and high triplet host material for highly efficient blue thermally activated delayed fluorescent device. *ACS Appl. Mater. Interfaces* 11, 14909–14916. doi: 10.1021/acsmi.9b00931
- Ahn, D. H., Maeng, J. H., Lee, H., Yoo, Y., Lampande, R., Lee, J. Y., et al. (2020). Rigid oxygen-bridged boron-based blue thermally activated delayed fluorescence emitter for organic light emitting diode: approach towards satisfying high efficiency and long lifetime

- together. *Adv. Optical Mater.* 2000102. doi: 10.1002/adom.20200102
- Baldo, M. A., O'Brien, D. F., You, Y., Shoustikov, A., Sibley, S., Thompson, M. E., et al. (1998). Highly efficient phosphorescent emission from organic electroluminescent devices. *Nature* 395, 151–154. doi: 10.1038/25954
- Bonardi, L., Kanaan, H., Camerel, F., Jolinat, P., Retailleau, P., and Ziesler, R. (2008). Fine-tuning of yellow or red photo- and electroluminescence of functional difluoro-boradiazaindacene films. *Adv. Funct. Mater.* 18, 401–413. doi: 10.1002/adfm.200700697
- Brown, H. C., and Dodson, V. H. (1957). Studies in stereochemistry. XXII. the preparation and reactions of trimesitylborane. evidence for the non-localized nature of the odd electron in triarylborane radical ions and related free radicals. *J. Am. Chem. Soc.* 79, 2302–2306. doi: 10.1021/ja01566a076
- D'aléo, A., Sazzad, M. H., Kim, D. H., Choi, E. Y., Wu, J. W., Canard, G., et al. (2017). Boron difluoride hemicurcuminoid as an efficient far red to near-infrared emitter: toward OLEDs and laser dyes. *Chem. Commun.* 53, 7003–7006. doi: 10.1039/C7CC01786C
- Elbing, M., and Bazan, G. C. (2008). A new design strategy for organic optoelectronic materials by lateral boryl substitution. *Angew. Chem. Int. Ed.* 47, 834–838. doi: 10.1002/anie.200703722
- Entwistle, C. D., and Marder, T. B. (2004). Applications of three-coordinate organoboron compounds and polymers in optoelectronics. *Chem. Mater.* 16, 4574–4585. doi: 10.1021/cm0495717
- Fraith, D., Massue, J., Ulrich, G., and Ziesler, R. (2014). Luminescent materials: locking  $\pi$ -conjugated and heterocyclic ligands with boron(III). *Angew. Chem. Int. Ed.* 53, 2290–2310. doi: 10.1002/anie.201305554
- Han, S. H., Jeong, J. H., Yoo, J. W., and Lee, J. Y. (2019). Ideal blue thermally activated delayed fluorescence emission assisted by a thermally activated delayed fluorescence assistant dopant through a fast reverse intersystem crossing mediated cascade energy transfer process. *J. Mater. Chem. C* 7, 3082–3089. doi: 10.1039/C8TC06575F
- Hatakeyama, T., Shiren, K., Nakajima, K., Nomura, S., Nakatsuka, S., Kinoshita, K., et al. (2016). Ultrapure blue thermally activated delayed fluorescence molecules: efficient HOMO–LUMO separation by the multiple resonance effect. *Adv. Mater.* 28, 2777–2781. doi: 10.1002/adma.201505491
- Hirai, H., Nakajima, K., Nakatsuka, S., Shiren, K., Ni, J., Nomura, S., et al. (2015). One-step borylation of 1,3-diaryloxybenzenes towards efficient materials for organic light-emitting diodes. *Angew. Chem. Int. Ed.* 54, 13581–13585. doi: 10.1002/anie.201506335
- Im, Y., Byun, S. Y., Kim, J. H., Lee, D. R., Oh, C. S., Yook, K. S., et al. (2017). Recent progress in high-efficiency blue-light-emitting materials for organic light-emitting diodes. *Adv. Funct. Mater.* 27:1603007. doi: 10.1002/adfm.201603007
- Karthik, D., Ahn, D. H., Ryu, J. H., Lee, H., Maeng, J. H., Lee, J. Y., et al. (2020). Highly efficient blue thermally activated delayed fluorescence organic light emitting diodes based on tercarbazole donor and boron acceptor dyads. *J. Mater. Chem. C* 8, 2272–2279. doi: 10.1039/C9TC05950D
- Kim, K.-H., and Kim, J. J. (2018). Origin and control of orientation of phosphorescent and TADF dyes for high-efficiency OLEDs. *Adv. Mater.* 30:1705600. doi: 10.1002/adma.201705600
- Kim, K. J., Kim, G. H., Lampande, R., Ahn, D. H., Im, J. B., Moon, J. S., et al. (2018). A new rigid diindolocarbazole donor moiety for high quantum efficiency thermally activated delayed fluorescence emitter. *J. Mater. Chem. C* 6, 1343–1348. doi: 10.1039/C7TC04852A
- Kitamoto, Y., Namikawa, T., Ikemizu, D., Miyata, Y., Suzuki, T., Kita, H., et al. (2015). Light blue and green thermally activated delayed fluorescence from 10H-phenoxaborin-derivatives and their application to organic light-emitting diodes. *J. Mater. Chem. C* 3, 9122–9130. doi: 10.1039/C5TC01380A
- Kitamoto, Y., Namikawa, T., Suzuki, T., Miyata, Y., Kita, H., Sato, T., et al. (2016). Dimesitylarylborane-based luminescent emitters exhibiting highly-efficient thermally activated delayed fluorescence for organic light-emitting diodes. *Org. Electron.* 34, 208–217. doi: 10.1016/j.orgel.2016.04.030
- Kondo, Y., Yoshiura, K., Kitera, S., Nishi, H., Oda, S., Gotoh, H., et al. (2019). Narrowband deep-blue organic light-emitting diode featuring an organoboron-based emitter. *Nat. Photonics* 13, 678–682. doi: 10.1038/s41566-019-0476-5
- Lee, Y. H., Park, S., Oh, J., Shin, J. W., Jung, J., Yoo, S., et al. (2017). Rigidity-induced delayed fluorescence by ortho donor-appended triarylboron compounds: record-high efficiency in pure blue fluorescent organic light-emitting diodes. *ACS Appl. Mater. Interfaces* 9, 24035–24042. doi: 10.1021/acsami.7b05615
- Lee, Y. H., Park, S., Oh, J., Woo, S.-J., Kumar, A., Kim, J.-J., et al. (2018). High-efficiency sky blue to ultradeep blue thermally activated delayed fluorescent diodes based on ortho-carbazole-appended triarylboron emitters: above 32% external quantum efficiency in blue devices. *Adv. Opt. Mater.* 6:1800385. doi: 10.1002/adom.201800385
- Li, G., Lou, W., Wang, D., Deng, C., and Zhang, Q. (2019). Difluoroboron-enabled thermally activated delayed fluorescence. *ACS Appl. Mater. Interfaces* 11, 32209–32217. doi: 10.1021/acsami.9b08107
- Li, P., Chan, H., Lai, S.-L., Ng, M., Chan, M.-Y., and Yam, V. W.-W. (2019). Four-coordinate boron emitters with tridentate chelating ligand for efficient and stable thermally activated delayed fluorescence organic light-emitting devices. *Angew. Chem. Int. Ed.* 58, 9088–9094. doi: 10.1002/anie.201903332
- Liang, X., Tu, Z.-L., and Zheng, Y.-X. (2019). Thermally activated delayed fluorescence materials: towards realization of high efficiency through strategic small molecular design. *Chem. A Eur. J.* 25, 5623–5642. doi: 10.1002/chem.201805952
- Liang, X., Yan, Z.-P., Han, H.-B., Wu, Z.-G., Zheng, Y.-X., Meng, H., et al. (2018). Peripheral amplification of multi-resonance induced thermally activated delayed fluorescence for highly efficient OLEDs. *Angew. Chem. Int. Ed.* 57, 11316–11320. doi: 10.1002/anie.201806323
- Matsui, K., Oda, S., Yoshiura, K., Nakajima, K., Yasuda, N., and Hatakeyama, T. (2018). One-shot multiple borylation toward BN-doped nanographenes. *J. Am. Chem. Soc.* 140, 1195–1198. doi: 10.1021/jacs.7b10578
- Matsuo, K., and Yasuda, T. (2019). Boronate- and borinate-based  $\pi$ -systems for blue thermally activated delayed fluorescence materials. *Chem. Commun.* 55, 2501–2504. doi: 10.1039/C8CC10282A
- Mellerup, S. K., and Wang, S. (2019). Boron-doped molecules for optoelectronics. *Trends Chem.* 1, 77–89. doi: 10.1016/j.trechm.2019.01.003
- Meng, G., Chen, X., Wang, X., Wang, N., Peng, T., and Wang, S. (2019). Isomeric bright sky-blue TADF emitters based on bisacridine decorated DBNA: impact of donor locations on luminescent and electroluminescent properties. *Adv. Opt. Mater.* 7:1900130. doi: 10.1002/adom.201900130
- Nguyen, T. B., Nakanotani, H., Hatakeyama, T., and Adachi, C. (2020). The role of reverse intersystem crossing using a TADF-type acceptor molecule on the device stability of exciplex-based organic light-emitting diodes. *Adv. Mater.* 32:1906614. doi: 10.1002/adma.201906614
- Numata, M., Yasuda, T., and Adachi, C. (2015). High efficiency pure blue thermally activated delayed fluorescence molecules having 10H-phenoxaborin and acridan units. *Chem. Commun.* 51, 9443–9446. doi: 10.1039/C5CC0307E
- Oda, S., Kawakami, B., Kawasumi, R., Okita, R., and Hatakeyama, T. (2019). Multiple resonance effect-induced sky-blue thermally activated delayed fluorescence with a narrow emission band. *Org. Lett.* 21, 9311–9314. doi: 10.1021/acs.orglett.9b03342
- Park, I. S., Matsuo, K., Aizawa, N., and Yasuda, T. (2018). High-performance dibenzoheteraborin-based thermally activated delayed fluorescence emitters: molecular architectonics for concurrently achieving narrowband emission and efficient triplet–singlet spin conversion. *Adv. Funct. Mater.* 28:1802031. doi: 10.1002/adfm.201802031
- Park, I. S., Numata, M., Adachi, C., and Yasuda, T. (2016). A phenazaborin-based high-efficiency blue delayed fluorescence material. *Bull. Chem. Soc. Jpn.* 89, 375–377. doi: 10.1246/bcsj.20150399
- Pershin, A., Hall, D., Lemaur, V., Sancho-Garcia, J.-C., Muccioli, L., Zysman-Colman, E., et al. (2019). Highly emissive excitons with reduced exchange energy in thermally activated delayed fluorescent molecules. *Nat. Commun.* 10:597. doi: 10.1038/s41467-019-08495-5
- Schellhammer, K. S., Li, T.-Y., Zeika, O., Körner, C., Leo, K., Ortmann, F., et al. (2017). Tuning near-infrared absorbing donor materials: a study of electronic, optical, and charge-transport properties of aza-BODIPYs. *Chem. Mater.* 29, 5525–5536. doi: 10.1021/acs.chemmater.7b00653
- Scholz, S., Kondakov, D., Lüssem, B., and Leo, K. (2015). Degradation mechanisms and reactions in organic light-emitting devices. *Chem. Rev.* 115, 8449–8503. doi: 10.1021/cr400704v
- Song, D., Yu, Y., Yue, L., Zhong, D., Zhang, Y., Yang, X., et al. (2019). Asymmetric thermally activated delayed fluorescence (TADF) emitters with 5,9-dioxo-13b-boranaphtho[3,2,1-de]anthracene (OBA) as the acceptor and

- highly efficient blue-emitting OLEDs. *J. Mater. Chem. C* 7, 11953–11963. doi: 10.1039/C9TC041115J
- Stachelek, P., Alsimaree, A. A., Alnoman, R. B., Harriman, A., and Knight, J. G. (2017). Thermally-activated, delayed fluorescence in O,B,O- and N,B,O-strapped boron dipyrromethene derivatives. *J. Phys. Chem. A* 121, 2096–2107. doi: 10.1021/acs.jpca.6b11131
- Suzuki, K., Kubo, S., Shizu, K., Fukushima, T., Wakamiya, A., Murata, Y., et al. (2015). Triarylboron-based fluorescent organic light-emitting diodes with external quantum efficiencies exceeding 20 %. *Angew. Chem. Int. Ed.* 54, 15231–15235. doi: 10.1002/anie.201508270
- Tang, C. W., and Vanslyke, S. A. (1987). Organic electroluminescent diodes. *Appl. Phys. Lett.* 51, 913–915. doi: 10.1063/1.98799
- Turkoglu, G., Cinar, M. E., and Ozturk, T. (2017). Triarylborane-based materials for OLED applications. *Molecules* 22:1522. doi: 10.3390/molecules22091522
- Uoyama, H., Goushi, K., Shizu, K., Nomura, H., and Adachi, C. (2012). Highly efficient organic light-emitting diodes from delayed fluorescence. *Nature* 492, 234–238. doi: 10.1038/nature11687
- Von Grotthuss, E., John, A., Kaese, T., and Wagner, M. (2018). Doping polycyclic aromatics with boron for superior performance in materials science and catalysis. *Asian J. Org. Chem.* 7, 37–53. doi: 10.1002/ajoc.201700495
- Yamaguchi, S., and Wakamiya, A. (2006). Boron as a key component for new  $\pi$ -electron materials. *Pure Appl. Chem.* 78, 1413–1424. doi: 10.1351/pac200678071413
- Yang, X., Guo, H., Liu, B., Zhao, J., Zhou, G., Wu, Z., et al. (2018). Diarylboron-based asymmetric red-emitting Ir(III) complex for solution-processed phosphorescent organic light-emitting diode with external quantum efficiency above 28%. *Adv. Sci.* 5:1701067. doi: 10.1002/advs.201800950
- Zampetti, A., Minotto, A., Squeo, B. M., Gregoriou, V. G., Allard, S., Scherf, U., et al. (2017). Highly efficient solid-state near-infrared organic light-emitting diodes incorporating A-D-A dyes based on  $\alpha,\beta$ -unsubstituted “BODIPY” moieties. *Sci. Rep.* 7:1611. doi: 10.1038/s41598-017-01785-2
- Zhang, Y., Zhang, D., Wei, J., Liu, Z., Lu, Y., and Duan, L. (2019). Multi-resonance induced thermally activated delayed fluorophores for narrowband green OLEDs. *Angew. Chem. Int. Ed.* 58, 16912–16917. doi: 10.1002/anie.201911266

**Conflict of Interest:** The authors declare that the research was conducted in the absence of any commercial or financial relationships that could be construed as a potential conflict of interest.

Copyright © 2020 Lee, Karthik, Lampande, Ryu and Kwon. This is an open-access article distributed under the terms of the Creative Commons Attribution License (CC BY). The use, distribution or reproduction in other forums is permitted, provided the original author(s) and the copyright owner(s) are credited and that the original publication in this journal is cited, in accordance with accepted academic practice. No use, distribution or reproduction is permitted which does not comply with these terms.